The thermal decomposition mechanism of zinc monosalicylates

Jutang Sun[*], Liangjie Yuan, Keli Zhang

Department of Chemistry, Wuhan University, Wuhan 430072, China

Abstract

α-Zn(o-OC$_6$H$_4$CO$_2$) and β-Zn(o-OC$_6$H$_4$CO$_2$) with different structures were synthesized by the rheological phase reaction method and thermal decomposition method, respectively. The TG, DTG and DTA curves were measured in N$_2$. α-Zn(o-OC$_6$H$_4$CO$_2$) at 409°C, β-Zn(o-OC$_6$H$_4$CO$_2$) at 375°C, started to decompose, and form zinc oxide, dibenzofuran, xanthene, xanthenone, 1,2-dibenzopyrone and 2-phenyl-1,2-dibenzopyran, etc. The products of thermal decomposition were characterized with infrared spectra, powder X-ray diffraction and gas chromatography and mass spectrography. The thermal decomposition reaction mechanism is discussed. © 1999 Elsevier Science B.V. All rights reserved.

1. Introduction

The thermal decomposition of the transition metal salicylates has been reported in air [1–3]. The organic products of thermal decomposition in air were burned above 350°C, the solid residues are mainly metal carbonates and oxides. However, no other detailed study has been reported on the thermal decomposition reaction mechanism of salicylates in inert atmosphere. In our previous works [4,5], it was found that many aromatic organic compounds, such as benzophenone and anthraquinone, were produced when the metal aromatic carboxylates were pyrolyzed in inert atmosphere. In this paper, zinc monosalicylates with different structures, α-ZnSal and β-ZnSal (Sal = o-OC$_6$H$_4$CO$_2$), were synthesized by the rheological phase reaction method and thermal decomposition

method. The products of thermal decomposition are characterized. The thermal decomposition reaction mechanism is investigated, and it is expected to obtain a new path of synthesizing aryl compounds.

2. Experimental

Preparation of samples: Salicylic acid and zinc oxide are analytical reagent grade. The salicylic acid and zinc oxide were fully mixed by grinding in 1 : 1 mole ratio, a proper amount of water was added, and prepared to solid–liquid rheological state (solid–liquid rheological state is a kind of semisolid in which solid particles and liquid substance were uniformly distributed). Then it was reacted for 2–4 h in a closed container at 70–90°C. That is, α-ZnSal (white powder) was synthesized by the use of the rheological phase reaction method. The pale yellow β-ZnSal was obtained by thermal decomposition of Zn(HOC$_6$H$_4$CO$_2$)$_2$ in Ar at 280°C for 4–5 h.

*Corresponding author. Fax: +86-27-87647617; e-mail: jtsun@whu.edu.cn

The contents of carbon and hydrogen were determined by elemental analysis with a Perkin-Elmer 240B analyzer, and the zinc contents were determined by EDTA titration. The experimental data (for α-ZnSal: Zn 32.60, C 41.54, H 2.05%, for β-ZnSal: Zn 32.25, C 41.66, H 2.15%) agree with the calculated values (Zn 32.45, C 41.73, H 2.00%).

Thermal analysis and collection of pyrolysis products: The TG, DTG (13.09 and 10.05 mg sample) and DTA (10 mg sample) curves of α- and β-ZnSal were recorded with a Shimadzu DT-40 thermal analyzer in N_2 (flow rate 40 ml/min) at a heating rate of 20°C/min from room temperature to 900°C. In addition, the samples (2 g) were pyrolyzed by employing apparatus shown in the literature [5] in Ar (flow rate 100 ml/min) at 450°C for 9 h, and the condensate of gas phase products was collected.

Analysis of pyrolysis products: The infrared spectra of the samples in KBr pellets were measured on a Nicolet 550 FT-IR spectrometer in the range of 4000 to 400 cm^{-1}. The X-ray diffraction pattern was obtained with a Rigaku D/MAX-RA model X-ray diffractometer with a Ni-filter and graphite monochromator, and Cu Kα_1 radiation ($\lambda = 0.15405$ nm). Gas chromatography–mass spectrometry (GC–MS) was carried out with a HP 5790A gas chromatograph, J&W Science DB-5 elastic quartz capillary column (0.315 mm in inside diameter and 30 m in length) and VG 7070E-HF double focusing magneto mass spectrometer. Gas chromatography: the carrier gas is He, pre-column pressure 10 kg/cm^2, starting temperature 50°C, heating rate 8°C/min, final temperature 290°C, GC–MS interface temperature 250°C. Mass spectrometry: resolution is 1000, EI ion source, ion source temperature 200°C, accelerating voltage 6 kV, electron energy 70 eV, scanning range 45–800 m/z.

3. Results and discussion

In the IR spectra of α-ZnSal (β-ZnSal), the sharp absorption bands at 1612 (1617), 1580 (1584), 1479 (1480), 1450 (1452) cm^{-1} can be assigned to the C–C stretching vibrations of the benzene ring, and the strong bands at 1233 (1239) cm^{-1} to the C–O bands. The broad and very strong bands at 1531 (1545) cm^{-1} and 1421 (1425) cm^{-1} are due to the asymmetric and symmetric stretching vibration bands of the OCO. The
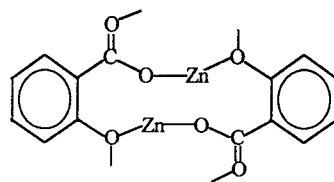

Fig. 1. The coordination structure unit in α- and β-Zn(o-OC$_6$H$_4$CO$_2$).

separation of the asymmetric and symmetric stretching vibration bands ($\nu_{as} - \nu_s$) of the OCO group is small. It is revealed that the carboxylate group is coordinated by a symmetric bidentate bridging with Zn^{2+} ion. The IR spectrum of β-ZnSal is consistent with that in the literature [2]. The recent study on the luminescence of α- and β-ZnSal demonstrated they had different structure [6].

The result of structure analysis indicated that the crystal structures belong to the monoclinic system. The lattice parameters of α-ZnSal are $a = 1.1655$, $b = 0.5359$, $c = 0.4999$ nm, $\beta = 98.65°$ and $Z = 2$. The lattice parameters of β-ZnSal are $a = 2.4425$, $b = 0.7004$, $c = 0.7615$ nm, $\beta = 93.88°$ and $Z = 8$. But, in both α-ZnSal and β-ZnSal, there is the coordination structure unit as shown in Fig. 1.

Fig. 2 shows the DTA, TG and DTG curves of α- and β-ZnSal. On the DTA curves of both, an endothermic peak is observed at 462°C and 498°C, respectively. The TG curves have two stages: For α-ZnSal, in first stage, the weight loss is 50.71% at 409–516°C, next, it has a slow weight loss at 550–890°C, the value is 6.01%. For β-ZnSal, the weight loss is 46.64% at 375–545°C, and 10.16% at 545–890°C. The total weight losses for α- and β-ZnSal are 56.72% and 56.80%, respectively. The black solid residue is a mixture of zinc oxide and carbon. So the thermal decomposition reaction can be considered as follows:

$$2Zn(OC_6H_4CO_2) \overset{450°C}{\underset{Ar}{\rightarrow}} 2ZnO + C +$$

$$\text{gas phase products} \uparrow \qquad (1)$$
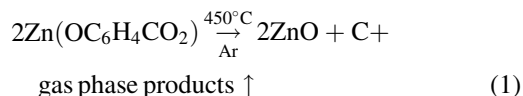
The calculated weight loss (56.63%) according to Eq. (1) agreed with the above found values.

When α- and β-ZnSal were decomposed at 450°C in Ar, CO_2 was detected in the gas products by means of chemical method. In the powder X-ray diffraction patterns of the solid residues, the diffraction lines of ZnO appeared only, the interplanar spacing values are
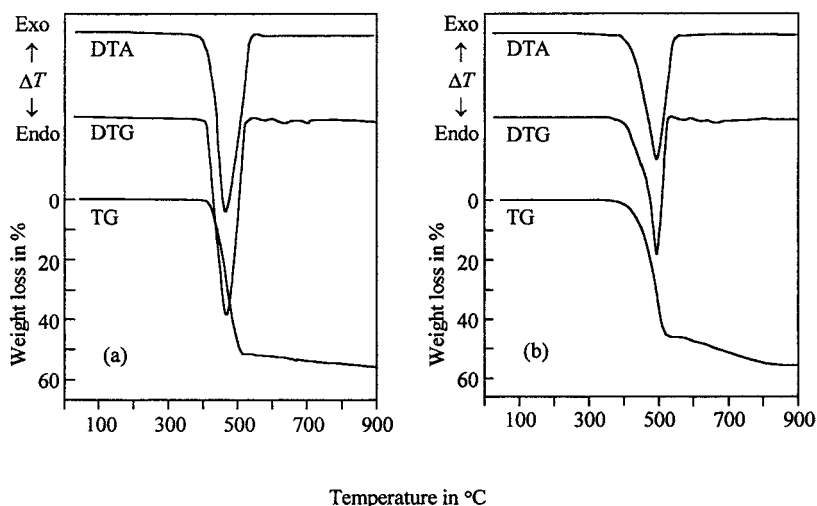
Fig. 2. TG, DTG and DTA curves for the thermal decomposition of (a) α-Zn(o-OC$_6$H$_4$CO$_2$) and (b) β-Zn(o-OC$_6$H$_4$CO$_2$) in N$_2$.

0.2820, 0.2608, 0.2479, 0.1914 and 0.1626 nm. They are corresponding to the (1 0 0), (0 0 2), (1 0 1) and (1 1 0) planes of zinc oxide with hexagonal wurtzite structure. The calculated cell parameters are $a = 0.3256$, $c = 0.5215$ nm.

The condensate of the gas phase products is a dark red thick matter. The results of GC–MS analysis are presented in Table 1. The main components are dibenzofuran, xanthene, xanthenone, 1,2-dibenzopyrone and 2-phenyl-1,2-dibenzopyran. The colorless crystal of xanthenone was obtained by washing the condensed products with absolute alcohol, and the infrared spectrum (Fig. 3) is consistent with the standard spectrum (IR, Sadtler no.18091 K).

The above results revealed the thermal decomposition mechanism as follows.

During the thermal decomposition of zinc monosalicylates, the fracture of bonds occurs chiefly in accordance with Eqs. (2) and (3), and ·C$_6$H$_4$O·, ·C$_6$H$_4$C(O)· and :C$_6$H$_4$ free radicals were formed.

Table 1

GC–MS results of condensate of gas phase products for the thermal decomposition of α- and β-Zn(o-OC$_6$H$_4$CO$_2$) at 450°C in Ar

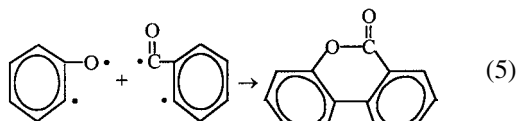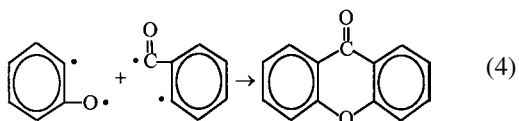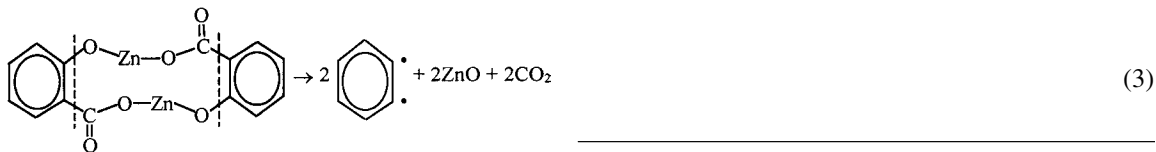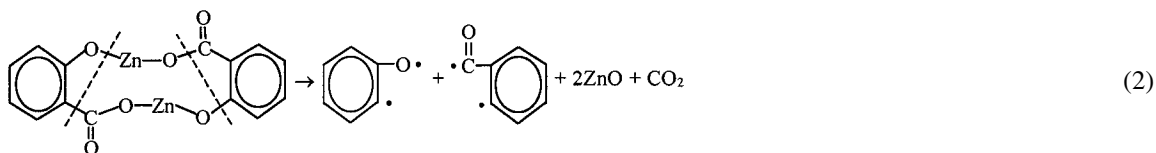| No.	α-Zn(o-OC$_6$H$_4$CO$_2$)		β-Zn(o-OC$_6$H$_4$CO$_2$)		Molecular weight	Compound
	Retention time (min)	Peak area (%)	Retention time (min)	Peak area (%)		
1	9.617	1.55	6.972	4.55	94	Phenol
2	18.585	0.31	14.553	0.73	154	Biphenyl
3	18.998	2.39	14.995	3.84	170	Diphenyl ether
4	21.476	23.97	17.430	24.92	168	Dibenzofuran
5	22.449	0.28	18.094	0.75	166	Fluorene
6	23.688	11.20	19.339	10.50	182	Xanthene
7	25.045	0.06	20.639	0.17	180	Fluorenone
8	27.346	37.57	22.521	29.01	196	Xanthenone
9	28.556	8.92	23.822	17.14	196	1,2-Dibenzopyrone
10	28.644	0.16	23.959	0.49	246	2-Phenoxy-biphenyl
11	30.857	0.22	25.675	0.13	242	9-Phenyl-fluorene
12	31.683	12.21	26.422	6.06	258	2-Phenyl-1,2-dibenzopyran
13	36.373	0.16	29.354	0.21	228	Triphenylene
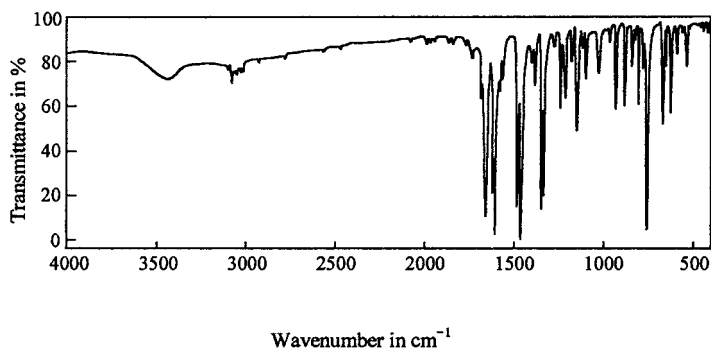
Fig. 3. Infrared spectrum of xanthenone separated from the condensate of gas phase products of the thermal decomposition of α- and β-Zn(o-OC$_6$H$_4$CO$_2$) at 450°C in Ar.

These free radicals reacted further to form xanthenone, 1,2-dibenzopyrone and dibenzofuran (4)–(6).

$$(2)$$

$$(3)$$

$$(4)$$

$$(5)$$

$$(6)$$

The :C$_6$H$_4$ free radical was further dehydrogenated to form carbon and H, and hydrogenated to form ·C$_6$H$_5$. The xanthene is the result from hydrogenating reduction of xanthenone. 1,2-Dibenzopyrone reacted with H and ·C$_6$H$_5$, and ·C$_6$H$_4$O· with H to produce 2-phenyl-1,2-dibenzopyran and phenol, respectively.

A small amount of triphenylene contained in the products demonstrates the formation of :C$_6$H$_4$ in the course of the thermal decomposition. The triphenylene is a result of polymerizing from three :C$_6$H$_4$ (reaction (7)).

$$(7)$$
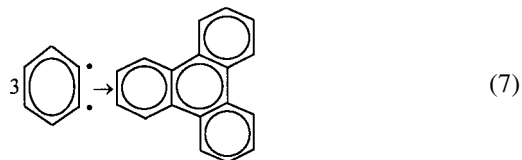
In addition, the foregoing free radicals can also interreact to form fluorenone, biphenyl, diphenyl ether, fluorene, 2-phenoxy-biphenyl and 9-phenyl-fluorene, etc. But the amount of these compounds is very small. This fact suggests that ·C$_6$H$_4$O·, ·C$_6$H$_4$C(O)· and :C$_6$H$_4$ free radicals did not enter the gas phase, the reactions forming xanthenone,

1,2-dibenzopyrone and dibenzofuran proceeded on the surface of solid products. That is to say, the fresh ZnO is probably a catalyst for some reactions. If the condition of thermal decomposition reaction can be exactly controlled, and the dehydrogenation is restrained, forming many by-products can be avoided.

Acknowledgements

References

[1] Y.Y. Kharitonov, Z.K. Tuiebakhova, Zh. Neorg, Khim. 31(8) (1986) 2005.

[2] J. Garcia-Oricain, A. Fuster Camps, J. Thermal Anal. 29(4) (1984) 793.

[3] Y.Y. Kharitonov, Z.K. Tuiebakhova, Zh. Neorg, Khim. 29(12) (1984) 3030.

[4] J.T. Sun, Z.H. Peng, X.Z. Du, Q.Y. Wang, Acta Chimica Sinica 49 (1991) 1094.

[5] J.T. Sun, K.L. Zhang, J.M. Zhang, Z.B. Qin, Y.L. Fen, Chem. J. Chinese Univ. 13 (1992) 1345.

[6] L.J. Yuan, Q.Y. Wang, J.T. Sun, Spectr. Lett. 31(8) (1998) 1733.